Supplementary Material

Molecular dynamics simulations of a characteristic DPC micelle in water

Stéphane Abel[¶*], *François-Yves Dupradeau*[§] *and Massimo Marchi*[¶]

[¶] Commissariat à l'Energie Atomique et aux Energies Alternatives, DSV/iBiTEC-S/SB2SM/LBMS, Saclay, France, CNRS UMR 8221, Saclay, France,

[§] Laboratoire des glucides, UFR de Pharmacie & CNRS FRE 3517, Université de Picardie - Jules Verne, Amiens, France.

* Corresponding author: stephane.abel@cea.fr

I. Molecular simulations of liquid n-tridecane.

Conformation and flexibility properties of the DPC alkyl chain were compared with n-tridecane (C13). Indeed, this alkane has an equivalent number of methylene groups and a methyl group at each end compared to DPC. 216 n-tridecane molecules were simulated in a cubic box using the AMBER99SB,[1] CHARMM36,[2] GROMOS53A6/54A7[3,4] and the GROMOS_Berger[5] force fields (named throughout as AMBER, CHARMM, GROMOS_53A6/54A7 and GROMOS-Berger). We carried out only a single simulation with the GROMOS53A6 and GROMOS54A7 force fields because the methylene and methyl groups are represented by identical bonded and non-bonded parameters in these force fields. The n-tridecane partial charges for the CHARMM36, GROMOS5354A7 and GROMOS-Berger simulations were directly taken from the respective force fields (Table S2). In case of n-tridecane modeled in the AMBER condition, we derived a new set of RESP charges by using the R.E.D. Server facility [6] and a similar protocol than that was previously reported for the DPC alkyl chain (i.e. "*all-trans dihedrals*" and two molecular orientations based on C_1, C_2, C_3 and C_3, C_2, C_1 atoms).

The simulations were carried out at T = 300 K and P = 1.015 bars during 10 ns after equilibration periods of 800 ps in NVT (200 ps) and NPT (500 ps) ensembles. In the AMBER and CHARMM simulation conditions, the same simulation protocol that that used for DPC was used (see the main text). For the GROMOS simulations, a twin-range cutoff scheme was used: interactions within a shorter-range cutoff (8 Å) were calculated at every step, whereas interactions were updated every 10 fs, together with the neighbor pair list with a longer cutoff (14 Å). The temperature and the pressure were kept fixed by using the Nosé-Hoover thermostat [7,8] and the Parrinello-Rahman barostat [9,10] with coupling constants of τ_T = 0.3 ps and τ_p = 1.0 ps, respectively. The time step was 2 fs and the P-LINCS algorithm [11] was used to restrain bond lengths to their equilibration values. Figure S2 provides final snapshots for the AMBER and GROMOS53A6/54A7 simulations.

Properties such as the density, molecular volume, isothermal compressibility, translational diffusion, the average percentage of the alkyl dihedral angles in the *trans* conformation and the mean dihedral transition time) were computed from the last 7 ns of each simulation with snapshots extracted every 2 ps and reported in Figure S3 and in Table S4.

Figures

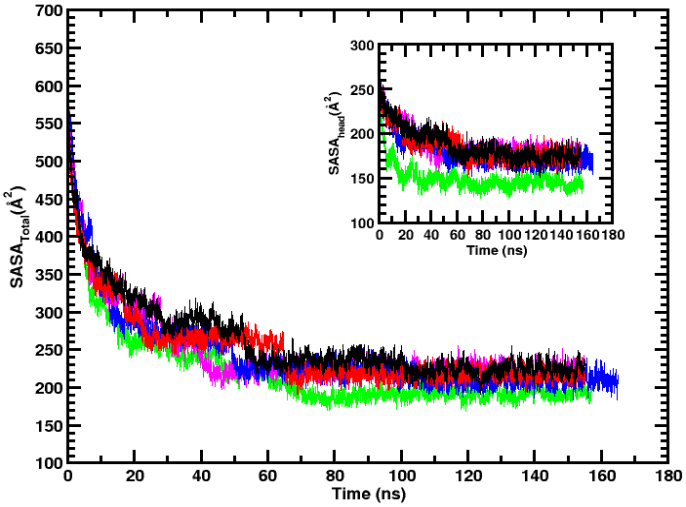

Figure S1: Time evolution of the solvent accessible surface area for the DPC monomer and the phosphocholine head group (inset) for the AMBER (black line), CHARMM (red line), GROMOS_53A6 (green line), GROMOS_54A7 (magenta) and GROMOS-Berger (blue line) simulations. See the main text for details.

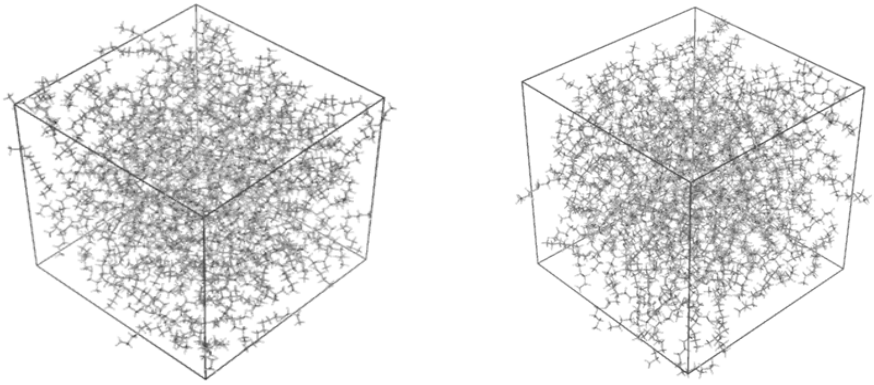

Figure S2: Final snapshots (t = 10 ns) of n-tridecane simulations at T = 300 K and P = 1.015 bars with the AMBER (left) and GROMOS53A6/54A7 (right) force fields.

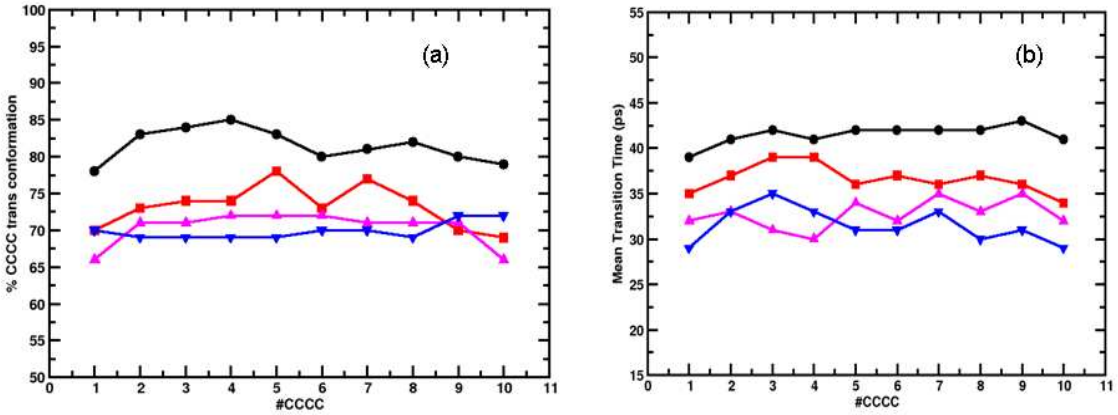

Figure S3: Average relative *trans* population for alkyl dihedral angles along the n-tridecane chain (a) and mean trans↔gauche transition time (b) for the AMBER (black and ●), CHARMM (red and ■), GROMOS_53A6/54A7 (magenta and ▲) and GROMOS-Berger (blue and ▼) simulations. Note that the first and last dihedral angle are $C_1C_2C_3C_4$ and $C_{10}C_{11}C_{12}C_{13}$, respectively. The statistical errors for the *trans* population and transition are less than 2 and 5 %, respectively.

Table

Force Field	AMBER		CHARMM		GROMOS_53A6		GROMOS_54A7		GROMOS_Berger	
Atom names	AT	qe^-	AT	qe^-	AT	qe^-	AT	qe^-	AT	qe^-
C1	CT	-0.1438	CTL5	-0.350	CH3	0.400	CH3p	0.400	LC3	0.400
H1A, H1B, H1C	HP	0.1235	HL	0.250	-	-	-	-	-	-
C2	CT	-0.1438	CTL5	-0.350	CH3	0.400	CH3p	0.400	LC3	0.400
H2A, H2B, H2C	HP	0.1235	HL	0.250	-	-	-	-	-	-
C3	CT	-0.1438	CTL5	-0.350	CH3	0.400	CH3p	0.400	LC3	0.400
H3A, H3B, H3C	HP	0.1235	HL	0.250	-	-	-	-	-	-
N4	N3	0.0290	NTL	-0.600	NL	-0.500	NL	-0.500	LNL	-0.500
C5	CT	-0.0360	CTL2	-0.100	CH2	0.300	CH2	0.300	LH2	0.300
H5A, H5B	HP	0.1324	HL	0.250	-	-	-	-	-	-
C6	CT	0.1414	CTL2	-0.080	CH2	0.400	CH2	0.400	LH2	0.400
H6A, H6B	H1	0.0548	HL	0.090	-	-	-	-	-	-
O7	OS	-0.5766	OSLP	-0.570	OA	-0.800	OA	-0.800	LOS	-0.800
P8	P	1.2266	PL	1.500	P	1.700	P	1.700	LP	1.700
O9, O10	O2	-0.7970	O2L	-0.780	OM	-0.800	OM	-0.800	LOM	-0.800
O11	OS	-0.5059	OSLP	-0.570	OA	-0.700	OA	-0.700	LOS	-0.700
C12	CT	0.1847	CTL2	-0.080	CH2	0.000	CH2	0.000	LP2	0.000
H12A, H12B	H1	0.0059	HAL2	0.090	-	-	-	-	-	-
C13	CT	0.0229	CTL2	-0.180	CH2	0.000	CH2	0.000	LP2	0.000
H13A, H13B	HC	0.0324	HAL2	0.090	-	-	-	-	-	-
C14	CT	-0.0182	CTL2	-0.180	CH2	0.000	CH2	0.000	LP2	0.000
H14A, H14B	HC	-0.0047	HAL2	0.090	-	-	-	-	-	-
C15	CT	0.0138	CTL2	-0.180	CH2	0.000	CH2	0.000	LP2	0.000
H15A, H15B	HC	-0.0121	HAL2	0.090	-	-	-	-	-	-
C16	CT	0.0351	CTL2	-0.180	CH2	0.000	CH2	0.000	LP2	0.000
H16A, H16B	HC	-0.0099	HAL2	0.090	-	-	-	-	-	-
C17	CT	0.0113	CTL2	-0.180	CH2	0.000	CH2	0.000	LP2	0.000
H17A, H17B	HC	-0.0043	HAL2	0.090	-	-	-	-	-	-
C18	CT	0.0169	CTL2	-0.180	CH2	0.000	CH2	0.000	LP2	0.000
H18A, H18B	HC	-0.0092	HAL2	0.090	-	-	-	-	-	-
C19	CT	0.0178	CTL2	-0.180	CH2	0.000	CH2	0.000	LP2	0.000
H19A, H19B	HC	-0.0101	HAL2	0.090	-	-	-	-	-	-
C20	CT	0.0105	CTL2	-0.180	CH2	0.000	CH2	0.000	LP2	0.000
H20A, H20B	HC	-0.0073	HAL2	0.090	-	-	-	-	-	-
C21	CT	0.0064	CTL2	-0.180	CH2	0.000	CH2	0.000	LP2	0.000
H21A, H21B	HC	0.0002	HAL2	0.090	-	-	-	-	-	-
C22	CT	0.0380	CTL2	-0.180	CH2	0.000	CH2	0.000	LP2	0.000
H22A, H22B	HC	-0.0042	HAL2	0.090	-	-	-	-	-	-
C23	CT	-0.0775	CTL3	-0.270	CH3	0.000	CH3p	0.000	LP3	0.000
H23A, H23B, H23C	HC	0.0153	HAL3	0.090	-	-	-	-	-	-

Table S1: Atom types (AT) and atomic charge values (qe^-) for DPC. Atom types are those defined in the Amber99SB, CHARMM36, GROMOS53A6, GROMOS54A7 and in the GROMOS_Berger force fields.

Force Field	AMBER		CHARMM		GROMOS		GROMOS_Berger	
Atom names	AT	qe$^-$	AT	qe$^-$	AT	qe$^-$	AT	qe$^-$
C1	CT	-0.0828	CTL2	-0.270	CH3/CH3p	0.00	LP2	0.00
H1A, H1B, H1C	H1	0.0165	HAL2	0.090	-	-	-	-
C2	CT	0.0398	CTL2	-0.180	CH2	0.00	LP2	0.00
H2A, H2B	HC	-0.0040	HAL2	0.090	-	-	-	-
C3	CT	0.0073	CTL2	-0.180	CH2	0.00	LP2	0.00
H3A, H3B	HC	-0.0001	HAL2	0.090	-	-	-	-
C4	CT	0.0085	CTL2	-0.180	CH2	0.00	LP2	0.00
H4A, H4B	HC	-0.0075	HAL2	0.090	-	-	-	-
C5	CT	0.0163	CTL2	-0.180	CH2	0.00	LP2	0.00
H5A, H5B	HC	-0.0097	HAL2	0.090	-	-	-	-
C6	CT	0.0233	CTL2	-0.180	CH2	0.00	LP2	0.00
H6A, H6B	HC	-0.0092	HAL2	0.090	-	-	-	-
C7	CT	0.0122	CTL2	-0.180	CH2	0.00	LP2	0.00
H7A, H7B	HC	-0.0070	HAL2	0.090	-	-	-	-
C8	CT	0.0233	CTL2	-0.180	CH2	0.00	LP2	0.00
H8A, H8B	HC	-0.0092	HAL2	0.090	-	-	-	-
C9	CT	0.0163	CTL2	-0.180	CH2	0.00	LP2	0.00
H9A, H9B	HC	-0.0097	HAL2	0.090	-	-	-	-
C10	CT	0.0085	CTL2	-0.180	CH2	0.00	LP2	0.00
H10A, H10B	HC	-0.0075	HAL2	0.090	-	-	-	-
C11	CT	0.0073	CTL2	-0.180	CH2	0.00	LP2	0.00
H12A, H11B	HC	-0.0001	HAL2	0.090	--	-	-	-
C12	CT	0.0398	CTL2	-0.180	CH2	0.00	LP2	0.00
H12A, H12B	HC	-0.0040	HAL2	0.090	--	-	-	-
C13	CT	-0.0828	CTL2	-0.270	CH3/CH3p	0.00	LP3	0.00
H12A, H12B, H13C	HC	0.0165	HAL3	0.090	-	-	-	-

Table S2: Same legend as Table S1 for n-tridecane. Note that in GROMOS53A6, GROMOS54A7 the two atom types CH3 and CH3p use bonded and non bonded parameters.

Micelle	a_M	b_M	c_M	a_{HC}	b_{HC}	c_{HC}	l_{pl}
AMBER	24.3	21.7	19.6	13.2	11.6	10.4	10.1
CHARMM	23.6	21.5	19.6	13.1	11.6	10.3	9.9
GROMOS_53A6	24.6	21.4	19.0	14.5	12.0	10. 2	9.4
GROMOS_54A7	24.4	21.9	19.9	13.4	11.7	10.3	10.2
GROMOS-Berger	24.0	21.4	19.3	13.8	11.8	10.2	9.6

Table S3: Average dimensions of the whole micelle and hydrophobic core in the different simulation conditions studied in this work. Values with M and HC subscripts were computed by including all the micelle atoms and those of the hydrophobic core of the inertia tensors, respectively. l_{pl} is the average head group thickness of the micelle in Å computed from the three semi-axes lengths. The statistical errors (maximum errors) are always lower than 0.9 and 0.4 Å for semi-axis lengths, and the head group thickness, respectively.

Force fields	AMBER	CHARMM	GROMOS_53A6/54A7	GROMOS_ Berger
ρ (g.cm^{-3})	0.748 ± 0.05	0.757 ± 0.056	0.764 ± 0.048	0.736 ± 0.057
exp.	0.750 [13,14]			
V_{mol} (Å^3)	408.8 ± 2 (408.3 ± 3.2)	404.4 ± 3.0 (404.4 ± 2.9)	(400.3 ± 2.9) (400.3 ± 2.6)	415.6 ± 3.2 (415.6 ± 3.3)
Exp	408.5 [2,13]			
β_T (10^{-10} Pa^{-1})	11.1 ± 0.2	11.6 ± 0.3	8.6 ± 0.3	13.3 ± 0.3
exp.sim.	10.0(10.7 - 11.5) [15,16]			
D_{trans} (10^{-10} m^2.s^{-1})	7.2 ± 0.3	10.1 ± 0.5	7.9 ± 0.5	15.1 ± 0.7
exp.	7.1 – 8.0 [17,18]			
%CCCC (%)	81.9 ± 0.2	73.6 ± 0.1	70.7 ± 0.1	70.2 ± 0.1
exp.	~ 68.0 [19]			

Table S4: Structural properties obtained for simulations of bulk n-tridecane at 300 K and P = 1.015 bars. ρ, V_{mol}, β_T , D_{trans} and %CCCC are the average density, the molecular volume, the isothermal compressibility, the translational diffusion and the relative population for the alkyl dihedral angles in the *trans* conformation (i.e. defined as $-60^o < \Phi < +60^o$), respectively. V_{mol} values were computed by dividing the average box volume by the number of n-tridecane molecules and with the *trjVoronoi* program (in parenthesis).[12]

References

(1) Hornak, V.; Abel, R.; Okur, A.; Strockbine, B.; Roitberg, A.; Simmerling, C. Comparison of multiple Amber force fields and development of improved protein backbone parameters. *Proteins Struct. Funct.* **2006**, *65*, 712–725.

(2) Klauda, J. B.; Venable, R. M.; Freites, J. A.; O'Connor, J. W.; Tobias, D. J.; Mondragon-Ramirez, C.; Vorobyov, I.; MacKerell, A. D.; Pastor, R. W. Update of the CHARMM All-Atom Additive Force Field for Lipids: Validation on Six Lipid Types. *J. Phys. Chem. B* **2010**, *114*, 7830–7843.

(3) Poger, D.; Van Gunsteren, W. F.; Mark, A. E. A new force field for simulating phosphatidylcholine bilayers. *J. Comput. Chem.* **2010**, *31*, 1117–1125.

(4) Oostenbrink, C.; Soares, T. A.; van der Vegt, N. F. A.; van Gunsteren, W. F. Validation of the 53A6 GROMOS force field. *Eur. Biophys. J.* **2005**, *34*, 273–284.

(5) Berger, O.; Edholm, O.; Jähnig, F. Molecular dynamics simulations of a fluid bilayer of dipalmitoylphosphatidylcholine at full hydration, constant pressure, and constant temperature. *Biophys. J.* **1997**, *72*, 2002–2013.

(6) Vanquelef, E.; Simon, S.; Marquant, G.; Garcia, E.; Klimerak, G.; Delepine, J. C.; Cieplak, P.; Dupradeau, F.-Y. R.E.D. Server: a web service for deriving RESP and ESP charges and building force field libraries for new molecules and molecular fragments. *Nucleic Acids Res.* **2011**, *39*, W511–W517.

(7) Nosé, S. A molecular dynamics method for simulations in the canonical ensemble. *Mol. Phys.* **1984**, *52*, 255–268.

(8) Hoover, W. G. Canonical dynamics: Equilibrium phase-space distributions. *Phys. Rev. A* **1985**, *31*, 1695–1697.

(9) Parrinello, M.; Rahman, A. Polymorphic transitions in single crystals: A new molecular dynamics method. *J. Appl. Phys.* **1981**, *52*, 7182–7190.

(10) Rahman, A.; Stillinger, F. H. Molecular Dynamics Study of Liquid Water. *J. Chem. Phys.* **1971**, *55*, 3336–3359.

(11) Hess, B. P-LINCS: A Parallel Linear Constraint Solver for Molecular Simulation. *J. Chem. Theory Comput.* **2007**, *4*, 116–122.

(12) Marchi, M. trjVoronoi, is a computational tool written in C++, which uses the voro++ library (version 0.4.3) of C. H. Rycroft to implement the Voronoi tessellation for frames of a GROMACS trajectory. It can compute the Voronoi volume of any given atoms.

(13) Aminabhavi, T. M.; Patil, V. B.; Aralaguppi, M. I.; Ortego, J. D.; Hansen, K. C. Density and Refractive Index of the Binary Mixtures of Cyclohexane with Dodecane, Tridecane, Tetradecane, and Pentadecane at (298.15, 303.15, and 308.15) K. *J. Chem. Eng. Data* **1996**, *41*, 526–528.

(14) Hust, J. G.; Schramm, R. E. Density and crystallinity measurements of liquid and solid n-undecane, n-tridecane, and o-xylene from 200 to 350.deg.K. *J. Chem. Eng. Data* **1976**, *21*, 7–11.

(15) Cerdeiriña, C. A.; Tovar, C. A.; González-Salgado, D.; Carballo, E.; Romaní, L. Isobaric thermal expansivity and thermophysical characterization of liquids and liquid mixtures. *Phys. Chem. Chem. Phys.* **2001**, *3*, 5230–5236.

(16) Mansker, L. .; Criser, A. .; Jangkamolkulchat, A.; Luks, K. . The isothermal compressibility of n-paraffin at low pressure. *Chem. Eng. Commun.* **1987**, *57*, 87–93.

(17) Marbach, W.; Hertz, H. G. Self- and Mutual Diffusion Coefficients of some n-Alkanes at Elevated Temperatures and Pressures. *Zeitschrift für Physikalische Chemie* **1996**, *193*, 19–40.

(18) Tofts, P. S.; Lloyd, D.; Clark, C. A.; Barker, G. J.; Parker, G. J. M.; McConville, P.; Baldock, C.; Pope, J. M. Test liquids for quantitative MRI measurements of self-diffusion coefficient in vivo. *Magn. Reson. Med.* **2000**, *43*, 368–374.

(19) Holler, F.; Callis, J. B. Conformation of the hydrocarbon chains of sodium dodecyl sulfate molecules in micelles: an FTIR study. *J. Phys. Chem.* **1989**, *93*, 2053–2058.